

# C/EBP Homologous Binding Protein (CHOP) Underlies Neural Injury in Sleep Apnea Model

Yu-Ting Chou, MD<sup>1,2</sup>; Guanxia Zhan, MD<sup>3</sup>; Yan Zhu, MD<sup>3</sup>; Polina Fenik, BS<sup>3</sup>; Lori Panossian, MD<sup>3,4</sup>; YanPeng Li, MD<sup>3</sup>; Jing Zhang, MD<sup>5</sup>; Sigrid Veasey, MD<sup>3,4</sup>

<sup>1</sup>*Sleep Center and Department of Pulmonary and Critical Care Medicine, Chang Gung Memorial Hospital, Chiayi, Taiwan;* <sup>2</sup>*Graduate Institute of Clinical Medical Sciences, College of Medicine, Chang Gung University, and Chang Gung University of Science and Technology, Taoyuan, Taiwan;*

<sup>3</sup>*Center for Sleep and Circadian Neurobiology;* <sup>4</sup>*Department of Medicine, University of Pennsylvania School of Medicine, Philadelphia, PA;* <sup>5</sup>*Department of Pulmonary Medicine, Peking University First Hospital, Beijing, China*

**Study Objectives:** Obstructive sleep apnea (OSA) is associated with cognitive impairment and neuronal injury. Long-term exposure to intermittent hypoxia (LTIH) in rodents, modeling the oxygenation patterns in sleep apnea, results in NADPH oxidase 2 (Nox2) oxidative injury to many neuronal populations. Brainstem motoneurons susceptible to LTIH injury show uncompensated endoplasmic reticulum stress responses with increased (CCAAT/enhancer binding protein homologous protein (CHOP). We hypothesized that CHOP underlies LTIH oxidative injury. In this series of studies, we first determined whether CHOP is upregulated in other brain regions susceptible to LTIH oxidative Nox2 injury and then determined whether CHOP plays an adaptive or injurious role in the LTIH response. To integrate these findings with previous studies examining LTIH neural injury, we examined the role of CHOP in Nox2, hypoxia-inducible factor-1 $\alpha$  (HIF-1 $\alpha$ ) responses, oxidative injury and apoptosis, and neuron loss.

**Design:** Within/between mice subjects.

**Setting:** Laboratory setting.

**Participants/Subjects:** CHOP null and wild-type adult male mice.

**Interventions:** LTIH or sham LTIH.

**Measurements and Main Results:** Relative to wild-type mice, CHOP<sup>-/-</sup> mice conferred resistance to oxidative stress (superoxide production/carbonyl proteins) in brain regions examined: cortex, hippocampus, and motor nuclei. CHOP deletion prevented LTIH upregulation of Nox2 and HIF-1 $\alpha$  in the hippocampus, cortex, and brainstem motoneurons and protected mice from neuronal apoptosis and motoneuron loss.

**Conclusions:** Endogenous CHOP is necessary for LTIH-induced HIF-1 $\alpha$ , Nox2 upregulation, and oxidative stress; CHOP influences LTIH-induced apoptosis in neurons and loss of neurons. Findings support the concept that minimizing CHOP may provide neuroprotection in OSA.

**Keywords:** Hypoxia, reoxygenation, unfolded protein response, PERK, GADD153 and gp91<sup>phox</sup>

**Citation:** Chou YT; Zhan G; Zhu Y; Fenik P; Panossian L; Li YanPeng; Zhang J; Veasey S. C/EBP homologous binding protein (CHOP) underlies neural injury in sleep apnea model. *SLEEP* 2013;36(4):481-492.

## INTRODUCTION

Obstructive sleep apnea (OSA) is associated with neurobehavioral impairments and nerve injury.<sup>1-5</sup> The pathophysiology of OSA involves frequent repeated sleep state-dependent collapse of the upper airway resulting in arterial oxygen desaturations and hypercapnia.<sup>6</sup> Awakening from sleep results in rapid restoration of pharyngeal patency and gas exchange. These cyclical events are repeated throughout sleep.<sup>6</sup> Degeneration of motor nerve axons can be found in soft palate tissue excised from individuals with OSA, but until recently, this nerve injury was thought largely to be a consequence of vibratory trauma from snoring.<sup>4,7-9</sup> However, the presence of neurogenic changes, neural injury and nerve dysfunction in OSA can be predicted, in part, by the severity of fluctuations in arterial oxygenation across apneic events.<sup>1,10</sup> Moreover, peripheral nerve conduction abnormalities in OSA extend beyond pharyngeal nerves.<sup>2,11,12</sup> Specifically, sural nerve action potential amplitudes are significantly reduced in individuals with OSA and are partially reversed upon effective treatment for OSA, supporting a direct role for OSA in peripheral nerve injury.<sup>13</sup>

Animal models implementing long-term intermittent hypoxia (LTIH), modeling sleep apnea arterial oxygenation patterns without snoring confounds, have been instrumental in determining what neural injuries may be caused or influenced by hypoxia/reoxygenation events of OSA and the mechanisms by which LTIH injures neural tissue. In rats, we have found that LTIH attenuates hypoglossal nerve amplitude responses to excitatory neurochemicals glutamate and serotonin.<sup>14</sup> Oxidative stress contributes to LTIH-reduced hypoglossal excitation, as superoxide dismutase mimetic administration across LTIH improves but does not normalize both hypoglossal excitatory responses and oxidative stress.<sup>14</sup> We have identified NADPH oxidase subtype 2 (Nox2) as a major source of oxidative stress and neuronal injury in LTIH.<sup>15</sup> Transgenic absence of Nox2 confers resistance to many of the LTIH injuries and neurobehavioral sequelae.<sup>15-20</sup> At the same time, hypoglossal, facial, and trigeminal motoneurons manifest increased endoplasmic reticulum (ER) stress in response to LTIH, including upregulation and activation of CCAAT-enhancer binding protein (C/EBP) homologous protein (CHOP).<sup>21</sup> The presence of CHOP in brainstem motoneurons in mice exposed to LTIH predicts activation of caspase-7 and -3.<sup>21</sup> CHOP, however, has been shown to contribute to both protective and injurious responses.<sup>22-25</sup> Thus, major questions at present include whether CHOP influences LTIH oxidative stress, and/or Nox2 activation and apoptosis in motoneurons.

We hypothesized that CHOP upregulates Nox2 oxidative injuries in LTIH. To define CHOP's role in LTIH injury and Nox2

Submitted for publication June, 2012

Submitted in final revised form August, 2012

Accepted for publication August, 2012

Address correspondence to: Sigrid C. Veasey, University of Pennsylvania, Translational Research Bldg., 125 S. 31<sup>st</sup> St., Philadelphia, PA; Tel: (215) 746-4801; Fax: (215) 746-4814; E-mail: [veasey@mail.med.upenn.edu](mailto:veasey@mail.med.upenn.edu)

**Table 1**—Antibodies used in immunohistology and western studies

Primary Antibody	Catalog # / Company	IF Dilution	WB Dilution	WB Band Size
$\alpha$ -tubulin (for HIF-1 $\alpha$ )	#2144 / Cell Signaling	—	1:1000	52 kDa
$\alpha$ -tubulin (for protein oxidation)	sc-8035 / Santa Cruz		1:1000	55 kDa
CHOP	sc-793 / Santa Cruz	1:100	—	—
Choline acetyltransferase	AB144P / Chemicon (Millipore)	1:1000	—	—
Cleaved caspase-3	#9661 / Cell Signaling	1:100	—	—
ERO1L	LS-C139777 / LifeSpan Biosciences	1:100	—	—
HIF-1 $\alpha$	NB 100-105 / Novus Biologicals	—	1:500	120 kDa
MAP-2	ab32454 / Abcam	1:500	—	—
Nox2 (gp91 <sup>phox</sup> )	611414 / BD Transduction Laboratories	1:500	—	—

upregulation in motoneurons, we examined oxidative and apoptosis/neuronal loss responses in motoneurons of mice with deletion of CHOP and wild-type controls. To relate these findings in motoneurons and motor nuclei with other neuronal groups susceptible to LTIH injury, we also examined CHOP relevance to LTIH oxidative injury in the cortex and hippocampus.

## METHODS

### Animals

Adult male B6.129S-*Ddit3<sup>tm1Dron</sup>/J* (CHOP<sup>-/-</sup>) mice bred > 10 generations onto C57BL/6J (B6), and B6 wild-type (WT) mice (Jackson Laboratory) were studied. Young adult CHOP<sup>-/-</sup> mice do not display any gross behavioral or physical abnormalities, and lifespan is similar to wild-type laboratory mice. All mice were 8–9 weeks (young adult) at the onset of intermittent hypoxia (IH) exposure. Mice were housed in groups of 5 mice/cage under conditions of 22 ± 1°C and 35% to 45% humidity and maintained on a 12-h light/dark cycle (with lights on at 6 a.m. and off at 6 p.m.). Food and water were provided *ad libitum*. The methods and study protocols were approved in full by the Institutional Animal Care and Use Committee of the University of Pennsylvania and conformed with the revised NIH Office of Laboratory Animal Welfare Policy.

### Intermittent Hypoxia Exposure

LTIH exposures were created by modulating flow rates and adjusting the balance of inspired nitrogen and oxygen in chambers using an automated nitrogen/oxygen delivery profile system (Oxycycler model A84XOV; Biospherix, Redfield, NY). The fraction of inspired oxygen (FIO<sub>2</sub>) declined from 21% to 5%, resulting in arterial oxyhemoglobin saturation nadir of 55% to 60% for < 5 seconds. A sham condition (Sham) controlled for chambers, fan, and air exchange noise, where mice were exposed continually to room air.<sup>14,16</sup> Exposures were conducted for 22–24 cycles/h, 10 h/day (07:00–17:00), and 7 days/week for either 4 or 12 weeks. The longer exposure was selected to examine apoptosis and superoxide production. Humidity, ambient CO<sub>2</sub>, and environmental temperature were held as for above cage environments.

### Tissue Procurement for Protein and RNA Studies

Immediately following LTIH and Sham exposures, mice designated for protein and RNA studies (n = 10/IH condition) were deeply anesthetized with pentobarbital (100 mg/kg intra-

peritoneally), and a transcardial perfusion with phospho-buffered saline and RNase inhibitor was performed. Brains were then rapidly removed, coronally sectioned on a cold (-20°C) platform into 1-mm slices for tissue punches of trigeminal, hypoglossal, and facial motor nuclei, rostral-dorsal hippocampus, and frontal cortex layers I–V. Punches were stored in -70°C before protein or RNA extraction. Because motor nuclei tissue samples in mice are small, specific motor nuclei were selected for either protein or mRNA studies.

### Western Blot

Western blot was used to compare Sham and LTIH redox responses in CHOP<sup>-/-</sup> and WT mice using tissue punches of pharyngeal motor nuclei and cortex, using previously reported protocols.<sup>26</sup> Individual tissue punches were homogenized on ice in lysis buffer with proteinase inhibitor cocktail. Purified protein was measured using the Pierce micro-BSA assay on centrifuged supernatants; 20  $\mu$ g of total protein was run on SDS-PAGE gels (10% Tris-HCL, Bio-Rad). Gels were transferred to polyvinylidene difluoride membranes and processed for detection of bands at the expected size. Details of primary antibodies are presented in Table 1. Images were analyzed with Odyssey Application software, version 3.0.16 (Li-Cor) to measure mean integrated densities. Data were normalized to the mean integrated density of  $\beta$ -tubulin in the same sample.

### Measurement of Protein Oxidation

Previous studies identified reduced carbonylated protein in Nox2<sup>-/-</sup> mice exposed to LTIH.<sup>15</sup> To test the hypothesis that endogenous CHOP influences carbonylation, motor trigeminal and cortex samples were used to detect protein carbonyls (n = 10 mice/group) for CHOP<sup>-/-</sup> and WT mice. To accomplish this, a protein oxidation detection kit was implemented according to the manufacturer's protocol, adding 2-mercaptoethanol to reduce reversible oxidative changes (Oxyblot, Millipore); 20  $\mu$ g protein/sample was incubated in 2,4-dinitrophenyl hydrazine (DNPH) for 15 min for derivatizing the carbonyl groups and then neutralized to stop the reaction.

### Quantitative Real-Time Polymerase Chain Reaction (PCR)

LTIH and Sham LTIH mice were deeply anesthetized before perfusing with PBS and RNAase inhibitor. Brains were then rapidly removed, coronally sectioned in a cold (-20°C) platform in 1-mm slices for tissue punches of the hypoglossal motor, cin-

gulate cortex, and CA1 hippocampus.<sup>26</sup> Total RNA was extracted using a Trizol and chloroform; 1 µg total RNA was subjected to reverse transcription using Superscript II RNase H (Gibco BRL, Invitrogen). Primer/probe sets were designed using Primer Express 2.0.0 software. Primers and probes using in this study are listed in Table 2. All primer probe sets showed excellent sensitivity and linearity (detection of > 10<sup>4</sup> copies/sample, r<sup>2</sup> > 0.99). Real-time PCR (7500 Real Time PCR System, Applied Biosystems) was performed in duplicate amplifying the cDNA at 50°C for 2 min, 95°C for 10 min, followed by 40 cycles of 15 s at 95°C, and 1 min at 60°C using TaqMan Gene Expression Master Mix (Applied Biosystems).

Copy numbers were determined from a standard generated for each primer/probe set with known copy numbers.

### Immunohistochemistry

Brainstem motoneurons were examined for the presence of Nox2, cleaved caspase-3 (CC-3), microtubule associate protein-2 (MAP-2), choline acetyltransferase (ChAT), and endoplasmic reticulum oxidoreductin-Ilike (ERO1L) in motor nuclei. Cortical (anterior cingulate and motor) and hippocampal neurons were examined for an LTIH effect on nuclear CHOP immunolabeling. Perfusion, cryopreservation, and sectioning details were recently published.<sup>21</sup> Details for primary antibodies used in these studies are presented in Table 1. Anti-ChAT was labeled with AlexaFluor594 (red) secondary, and other antibodies used to examine motoneurons were labeled with AlexaFluor488 (Invitrogen, green) for 1 h at room temperature.<sup>21</sup> For cortical and hippocampal CHOP immunolabeling, sections were labeled using blue alkaline phosphatase substrate (Vector Laboratories). Imaging was performed using a Leica SP5 with AOBs confocal taking 1-µm thick images, standardizing the imaging and coverslip distance per antigen series. NIH ImageJ was used to calculate the average optical density for target antigens in hypoglossal neurons. An observer blinded to experimental conditions and genotype measured immunointensity signals. All ChAT labeled neurons with visible nuclei were analyzed for CC-3 signals in nuclei and Nox2 signals in cytoplasm of ChAT-labeled motoneurons.

### Dihydroethidium Labeling and Analysis

Dihydroethidium is converted to fluorescent molecules dihydroethidium and ethidium, providing an index of superoxide production.<sup>27</sup> Groups of CHOP-/- and WT mice that had been exposed to 12 weeks of LTIH or Sham (n = 5/group) were given intraperitoneal injections of 30 mg/kg dihydroethidium (Anaspec) at 24 h and 6 h prior to perfusion. Brains and sections were processed as above. Hypoglossal motoneurons were imaged with a Leica SP-5 AOBs confocal microscope using a 546 laser tuned to 500-585 nm and a Texas red laser tuned to 605-700 nm; laser intensity, detector gain, am-

**Table 2**—Primer/probes sets for real time PCR

CHOP	NM_007837	Sense: CTCTGATCGACCGCATGGT (632-650) Anti-sense: AGTCCCCTCCTCAGCATGTG (777-758) Probe: AGCATGAACAGTGGGCATCACCTCC (663-687)
ERO1L	NM_015774.3	Sense: TGGTTTTACTCAGATTCATGGATTG (2275-2299) Anti-sense: TAAGCAAGGCTGAGGACACA (2410-2390) Probe: CCAGGACCTCAGTCATGCTGGGCT (2348-2371)
HIF-1α	NM_010431	Sense: CGA CCA CTG CTA AGG CAT CA (2260-2279) Anti-sense: TGA TTC AAA GTG GCA GAC AGC TT (2377-2355) Probe: CGG ACA GCC TCA CCA GAC AGA GCA (2283-2306)
Nox2	NM_007807.4	Sense: AAT GCC AAC TTC CTC AGC TAC AA (1482-1504) Anti-sense: AGT TGG GCC GTC CAT ACA GA (1620-1601) Probe: CTC AGG CCA ATC ACT TTG CTG TGC A (1531-1555)
Rn18S	NR_003278.2	Sense: GTA AGT GCG GGC CAT AAG CTT (1653-1674) Anti-sense: AGT CAA GTT CGA CCG TCT TCT CA (1787-1765) Probe: ACA CCG CCC GTC GCT ACT ACC GA (1697-1719)

plifier offset, and depth of the focal plane within the section were also standardized across all sections imaged to allow for semi-quantitative comparisons. Neurons within the hypoglossal nucleus > 30 µm in diameter were included in analysis using 2 mid-nucleus sections/mouse. ImageJ software was used with the readers blinded to LTIH and genotype conditions for each image to analyze immunodensities for each motoneuron averaged per mouse and analyzed in one-way ANOVA across the 4 groups.

### Motoneuron Morphology and Density Measures

The coronal cross-sectional area and number of motoneurons in the hypoglossal nucleus vary within animal across the rostral-caudal axis. Thus, a complete 1:3 series within the medulla was examined for each mouse with ChAT and MAP-2 labeling, and matching levels were confirmed for analysis. The number of motoneuron somata (cell diameter > 20 µm)<sup>28,29</sup> with visible nuclei within the hypoglossal nucleus to compare 4 groups: WT LTIH, WT Sham, CHOP-/- LTIH, and CHOP-/- Sham. All neurons with soma diameter > 20 µm showed both ChAT and MAP-2 labeling. The x,y coordinates of the cell counting box contained the entire coronal dimensions of the hypoglossal nucleus, and the z-dimensions were defined with differential interference contrast to include from 3 to 10 µm from the coverslip (z-movement resolution, 0.1 µm).<sup>16</sup> Cell count per box averaged per mouse was reported for n = 5 per genotype/IH condition with > 200 cells counted per mouse with investigators blinded to genotype/hypoxia conditions.

### Statistical Analysis

Data are presented as the mean (± standard error). One-way ANOVA was used for LTIH and Sham comparisons in WT only groups. Where multiple endpoints were examined together, Bonferroni comparison of selected groups was performed (Statview InStat 3 software). Two-way ANOVA with independent variables (genotype and hypoxia condition) was used to determine significant effect of CHOP-/- genotype or LTIH or both (GraphPrism 3.0cx software). All tests were two-tailed, and a final P-value less than 0.05 defined statistically significant results.

## RESULTS

### LTIH Upregulates CHOP in Many, But Not All, Brain Regions

Our previous study showed that motoneurons susceptible to LTIH induced injury evidenced higher nuclear CHOP expression in response to LTIH.<sup>21</sup> To extend these findings to other brain regions susceptible to LTIH, we examined the CHOP response to LTIH in the cortex and hippocampus, in addition to hypoglossal nucleus. Exposure to LTIH resulted in increased CHOP mRNA in the frontal cortex of wild-type mice ( $t = 5$ ,  $P < 0.01$ ) and an increase of similar magnitude in the hippocampus ( $t = 3$ ,  $P < 0.05$ ), as summarized in Figure 1A. CHOP mRNA increased ( $t = 6$ ,  $P < 0.0001$ ) more substantially in the hypoglossal nucleus (260% increase) compared to the cortex (67%) and hippocampus (74%). Consistent with the observed upregulation of CHOP mRNA, CHOP immunodensity increased significantly in each of these regions, as summarized in Figure 1B ( $P < 0.0001$ ). Across regions, the magnitude of LTIH immunolabeling changes was far greater than the LTIH effect on mRNA. The immunohistochemistry analysis focused only on pyramidal neurons, while micropunches included other neurons, glia, and surrounding tissue. Figure 1C shows representative examples of CHOP immunolabeling, highlighting weaker CHOP labeling in the pyramidal neurons in a Sham WT mouse with a greater CHOP labeling in the LTIH exposed mouse.

### Endogenous CHOP Contributes to Oxidative Stress in Regions Tested: the Hypoglossal Motor Nucleus and the Cortex

To test the hypothesis that superoxide production in LTIH is evident long term (12 wks) and to examine the role of CHOP in LTIH superoxide production in a representative group of motoneurons (hypoglossal motoneurons), we examined WT and CHOP<sup>-/-</sup> mice exposed to Sham or LTIH. Overall, there were specific significant genotype and hypoxia influences on DHE ( $P < 0.001$ ), as summarized in Figure 2A. While no difference in DHE expression in hypoglossal motoneurons was found between WT Sham and CHOP<sup>-/-</sup> Sham mice, in WT mice, there was a significant increase in DHE in hypoglossal motoneurons in LTIH compared to Sham WT ( $t = 6.2$ ,  $P < 0.001$ ). In contrast, there was no effect of LTIH on DHE in hypoglossal motoneurons in CHOP<sup>-/-</sup> mice. DHE in CHOP<sup>-/-</sup> mice exposed to LTIH was significantly less than in WT mice exposed to LTIH ( $t = 4.8$ ,  $P < 0.001$ ). Figure 2B provides an example of the DHE labeling. The DHE signal was highest in regions where strong CHOP was observed in response to LTIH in WT mice. In summary, LTIH results in a sustained increase in superoxide production in hypoglossal motoneurons, and endogenous CHOP positively influences this source of oxidative stress.

We next measured protein carbonylation across the 4 groups of mice for LTIH duration of 4 weeks ( $n = 10$  mice/group) in the trigeminal motor nucleus (where DHE labeling was similar to hypoglossal motoneurons) and in the frontal cortex to extend to another LTIH-vulnerable brain region. There were significant hypoxia and genotype influences on protein carbonylation for both motor trigeminal and cortex ( $P < 0.01$ ). There was a significant increase in protein oxidation in the motor trigeminal nucleus in WT LTIH compared to WT Sham ( $t = 3$ ,  $P < 0.05$ ) and a significant difference between WT LTIH and CHOP<sup>-/-</sup> LTIH ( $t = 3$ ,  $P < 0.05$ ) (Figure 3A, C). There was no significant

difference between CHOP<sup>-/-</sup> LTIH and CHOP<sup>-/-</sup> Sham mice. Similar relationships for LTIH and genotype were observed in the cortex and are presented in Figure 3B and D, where WT LTIH carbonylation compared to WT Sham was increased ( $t = 4$ ,  $P < 0.01$ ). Again, there was no significant difference between CHOP<sup>-/-</sup> LTIH and CHOP<sup>-/-</sup> Sham mice in the cortex. Thus, endogenous CHOP is necessary for the LTIH increase in carbonylation in both the trigeminal motor nucleus and cortex.

### LTIH Increases Nicotinamide Adenine Dinucleotide Phosphate Oxidase 2 (Nox2) in Hypoglossal Motoneurons in Wild-Type Mice, and Absence of CHOP Prevents the LTIH Induced Nox2 Upregulation in the Hypoglossal Nucleus

Previously we identified Nox2 as a major contributor to oxidative stress in catecholaminergic wake-active neurons in response to LTIH.<sup>15</sup> LTIH induced Nox2 upregulation in the hippocampus and cortex contributes to oxidative stress and related neurobehavioral impairments.<sup>30,31</sup> To test the hypothesis that Nox2 is also upregulated in motoneurons and the hippocampus in response to LTIH, we examined transcriptional and translational Nox2 in motoneurons and/or hippocampus in response to LTIH. Nox2 mRNA copy numbers in hypoglossal motoneurons ( $n = 5$ /group) were higher in WT LTIH mice relative to sham WT mice ( $t = 5$ ,  $P < 0.001$ ), as summarized in Figure 4A left bars. Similarly, Nox2 immunodensities in hypoglossal somata in WT mice increased in response to LTIH ( $t = 5$ ,  $P < 0.005$ ), as shown in Figure 4B left bars. Under sham conditions, very little Nox2 was evident in hypoglossal motoneurons, where most localized to the perinuclear region of motoneurons (Figure 4C). In contrast, in WT mice exposed to LTIH, Nox2 was evident in most, but not all, motoneurons within the hypoglossal nucleus. Nox2 was also increased in surrounding tissue within the hypoglossal nucleus, consistent with upregulation also in glia and in neuronal projections (Figure 4C).

Transgenic absence of CHOP prevented the LTIH-induced Nox2 upregulation in the 2 brain regions examined: the hippocampus and hypoglossal motoneurons. Specifically, in hypoglossal motoneurons, LTIH in CHOP<sup>-/-</sup> mice neither increased Nox2 mRNA (Figure 4A right bars) nor Nox2 immunodensity in XII motoneurons (Figure 4B right bars). There were similar LTIH and genotype effects in the hippocampus for Nox2 mRNA expression—WT LTIH was  $86 \pm 10$  vs. WT sham,  $147 \pm 17$  ( $t = 4$ ,  $P < 0.01$ ) Similarly, Nox2 immunodensity in the hippocampus increased in WT mice in LTIH—Sham WT,  $14 \pm 2$  vs LTIH WT,  $22 \pm 4$ ,  $t = 4$ ,  $P < 0.01$ ; and there was no increase in Nox2 in response to LTIH in CHOP<sup>-/-</sup> mice, CHOP<sup>-/-</sup> Sham— $9 \pm 1$  vs CHOP<sup>-/-</sup> LTIH,  $10 \pm 1$ ,  $t = 0.4$ , N.S. Nox2 immunoreactivity in the hippocampus in LTIH WT was greater than in CHOP<sup>-/-</sup> LTIH,  $t = 5$ ,  $P < 0.01$ . Thus, CHOP is necessary for LTIH-induced Nox2 upregulation of mRNA and protein in the hippocampus and hypoglossal nucleus.

### LTIH Increases Hypoxia-Inducible Factor-1 $\alpha$ (HIF-1 $\alpha$ ) in Hypoglossal Motoneurons in Wild-Type Mice, and Absence of CHOP Prevents the LTIH Induced HIF-1 $\alpha$ Upregulation

Previous work has shown that HIF-1 $\alpha$  is upregulated by LTIH *in vitro*, with similar changes in mRNA and protein, and that HIF-1 $\alpha$  may influence Nox2 upregulation in the cortex and brainstem in response to LTIH,<sup>32</sup> while Nox2 may influence

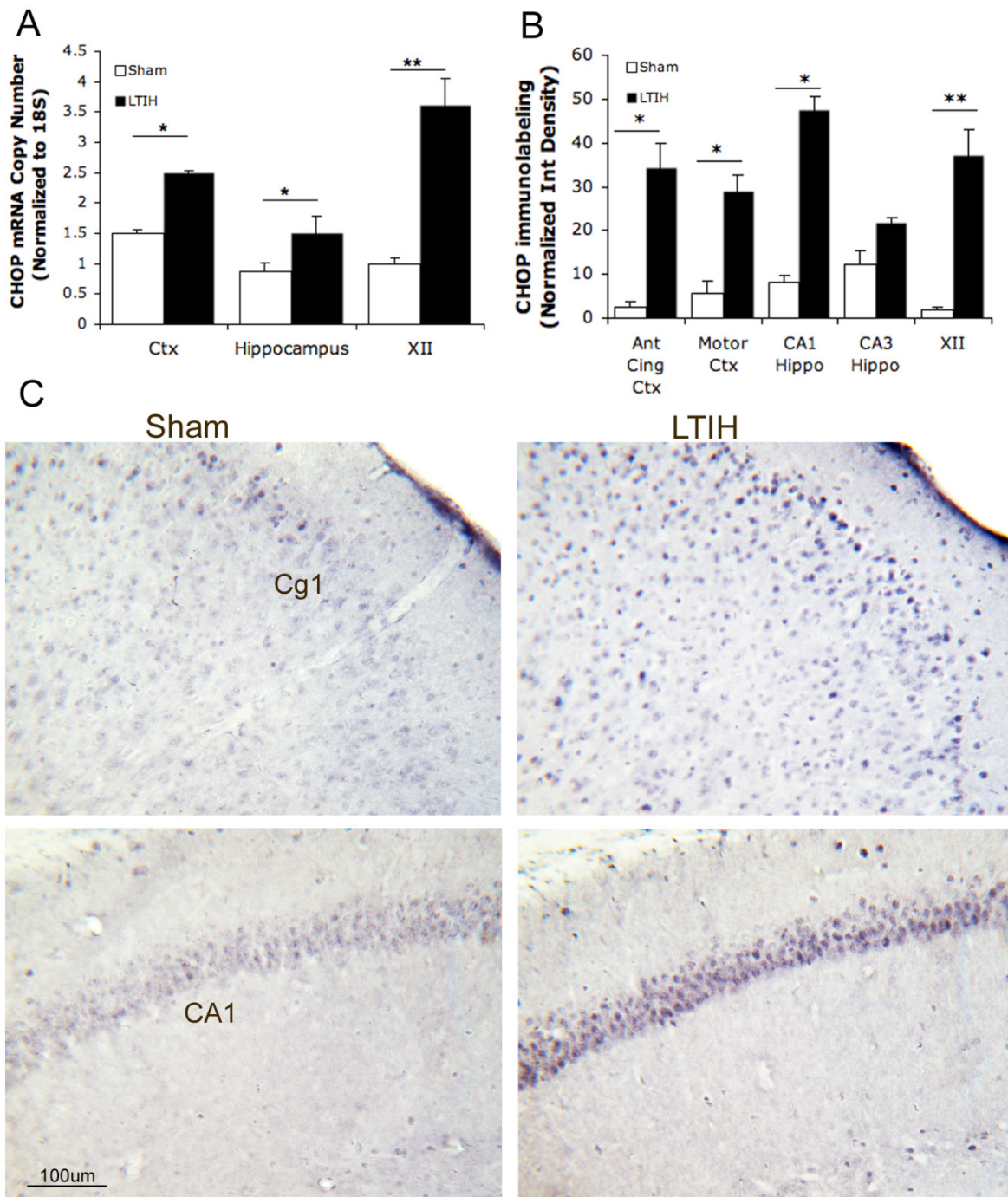


**Figure 1**—Long-term intermittent hypoxia (LTIH) increases endoplasmic stress protein, C/EBP homologous protein (CHOP) in pyramidal neurons in the cingulate cortex and hippocampus. **(A)** Mean CHOP mRNA relative normalized to ribosomal 18S in cortex, hippocampus and hypoglossal motoneurons after LTIH or Sham condition in wild-type mice. **(B)** Mean immunolabeling density of CHOP expressions in multiple brain regions after LTIH or Sham condition in wild-type mice, normalized to background immunointensity. **(C)** Representative images of CHOP immunohistochemistry staining in the cingulate 1 (Cg1) region of the cortex and CA1 region of the hippocampus in Sham and LTIH wild-type mice. Data presented as mean  $\pm$  SE. \* $P < 0.05$ ; \*\* $P < 0.01$ . Ctx, cortex; XII, hypoglossal motoneurons; Ant Cing Ctx, anterior cingulate cortex; Hippo, hippocampus.

HIF-1 $\alpha$  transcription.<sup>17</sup> To test the hypothesis that CHOP influences HIF-1 $\alpha$  responses to LTIH, we examined HIF-1 $\alpha$  transcriptional responses in hypoglossal motoneurons, cortex, and hippocampus in WT and CHOP $^{-/-}$  mice. Overall, there were significant genotype and LTIH condition effects on HIF-1 $\alpha$

mRNA in the hypoglossal nucleus. LTIH increased HIF-1 $\alpha$  in WT ( $t = 5.5$ ,  $P < 0.001$ ; Figure 5A). In contrast no difference was observed across LTIH conditions in CHOP $^{-/-}$  mice ( $t = 0.8$ , N.S). There was a significant difference between the HIF-1 $\alpha$  transcriptional response in WT LTIH compared to CHOP $^{-/-}$

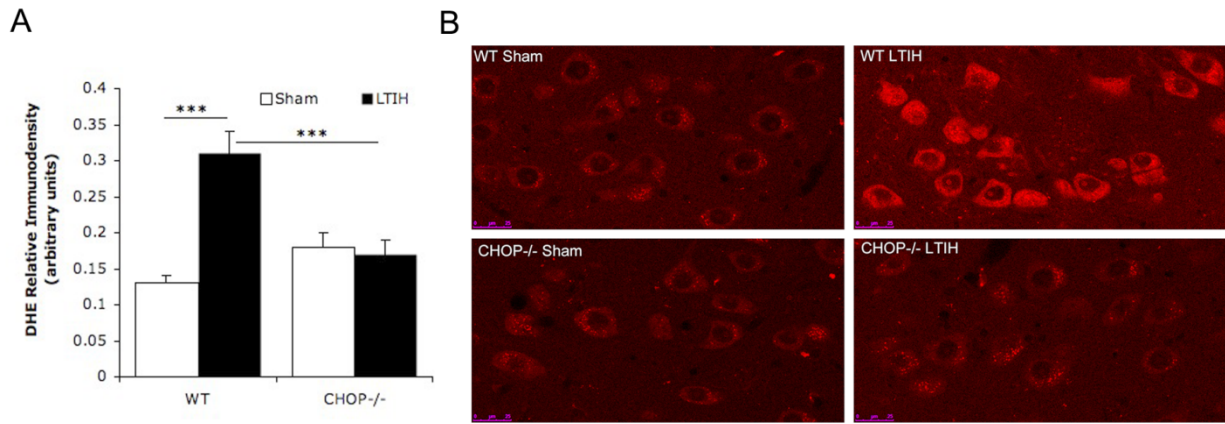


**Figure 2**—Endogenous CHOP is necessary for LTIH-induced superoxide production. Systemically-injected dihydroethidine converts to dihydroethidium (DHE) in the presence of superoxide and emits a fluorescence for excitation at 488 nm and emission at > 560 nm (red). **A**. Average fluorescence integrated densities of DHE in hypoglossal motoneurons from WT and CHOP knockout (CHOP<sup>-/-</sup>) mice after 12-weeks LTIH or sham LTIH exposure. **B**. Representative confocal images DHE fluorescence (red color) in large (> 25 μm) neurons in the XII nucleus of WT and CHOP<sup>-/-</sup> mice exposed to LTIH 12 wks or sham LTIH. Data presented as mean ± SE. P < 0.001.

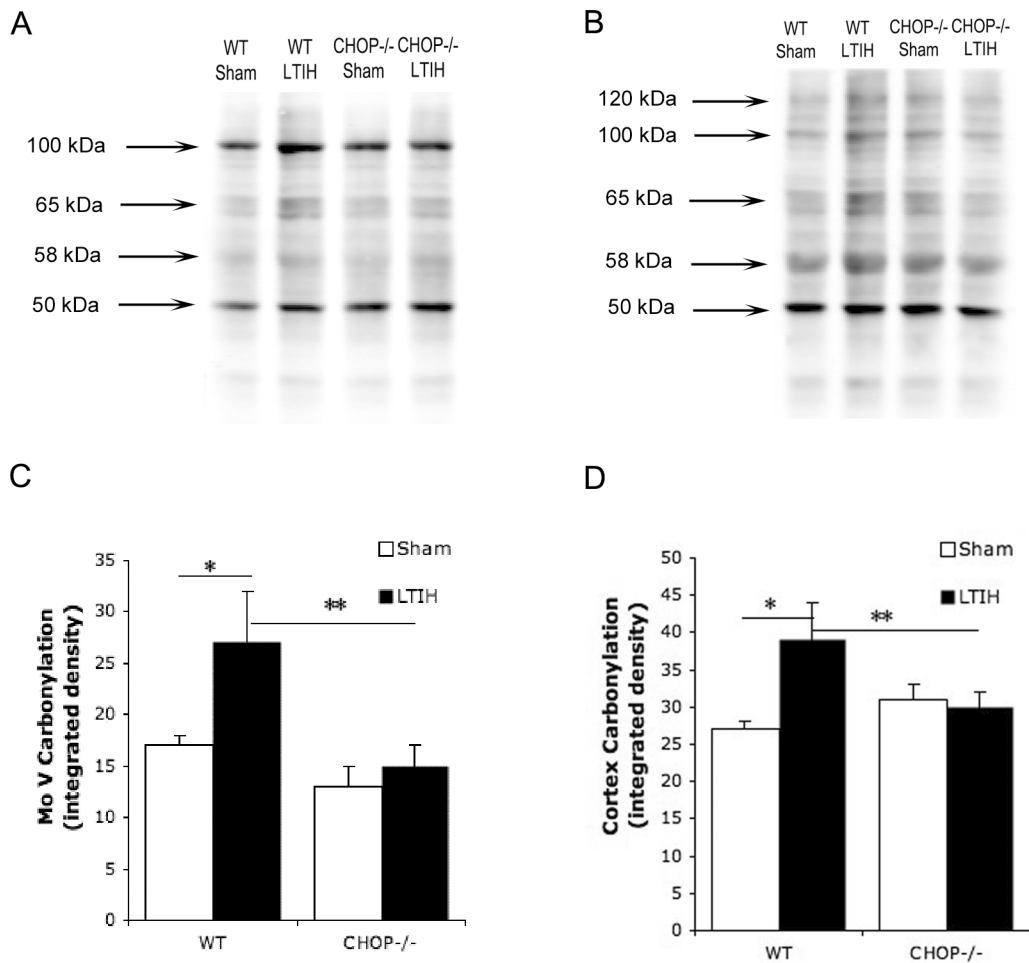


**Figure 3**—CHOP is necessary for LTIH protein oxidation in the brain. Representative western blot for carbonylated proteins in mo V (**A**) and cortex (**B**) from WT and CHOP<sup>-/-</sup> mice exposed to either LTIH or sham LTIH. Mean integrated immunodensities for carbonylated protein in trigeminal motoneurons (mo V) (**C**) and frontal cortex (**D**) between groups. Data presented as mean ± SE. \*P < 0.05; \*\*P < 0.01.

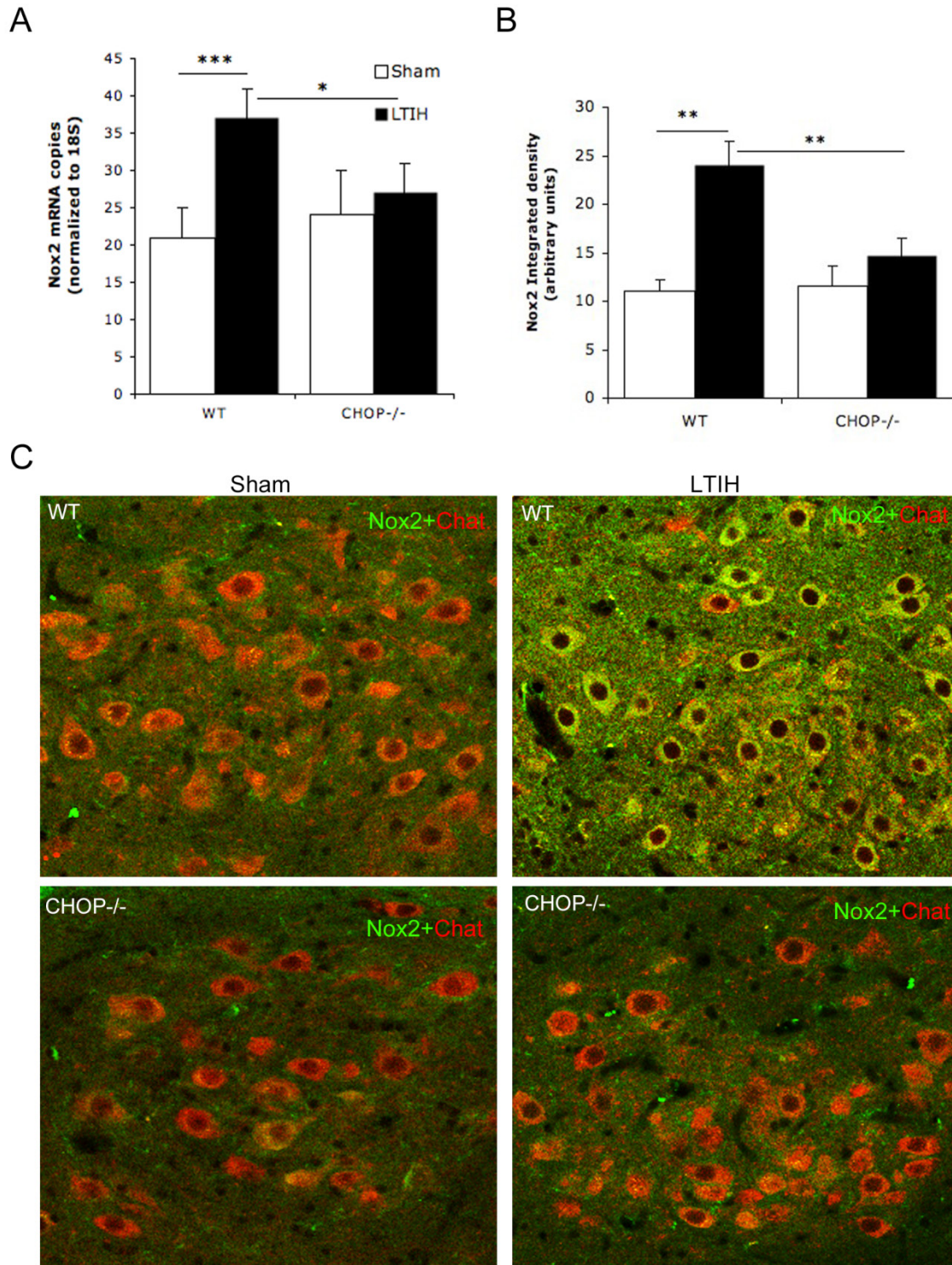


**Figure 4**—LTIH-induced upregulation of NADPH oxidase2 (Nox2) is prevented by transgenic absence of CHOP. **(A)** Nox2 mRNA expression in facial neurons in WT and CHOP<sup>-/-</sup> mice exposed to 4 weeks LTIH or sham LTIH. **(B)** Mean immunodensity for Nox2 expressions in hypoglossal motoneurons. **(C)** Sections of hypoglossal motoneurons with Nox2 (green) and ChAT (red) labeling. Nox2 was evident in most, but not all (see arrow), motoneurons within the hypoglossal nucleus in WT LTIH mice. In contrast, very little Nox2 was evident in WT sham LTIH and CHOP<sup>-/-</sup> mice under either condition. In WT LTIH mice, there were also higher Nox2 expressions in surrounding tissue with the hypoglossal neuron, consistent with upregulation also in glia and in neurites. Data are presented as mean  $\pm$  SE. \* $P < 0.05$ ; \*\* $P < 0.01$ ; \*\*\* $P < 0.001$ . ChAT, choline acetyltransferase.

LTIH ( $t = 3$ ,  $P < 0.05$ ). A similar response was observed for the hippocampus, where LTIH increased the HIF-1 $\alpha$  mRNA level in WT mice ( $t = 3$ ,  $P < 0.05$ ) but not in CHOP<sup>-/-</sup> mice (Figure 5A).

To determine whether the transcriptional response predicted a change in HIF-1 $\alpha$  protein, cortical tissue, for which we had sufficient quantities for both RNA and protein studies, was used: 50  $\mu$ g of protein was necessary to load to detect the 120-kDa band

## LTIH Increases an Additional Source of Oxidative Stress, Endoplasmic Reticulum Oxidoreductin-1L (ERO1L), and Endogenous CHOP is Necessary for ERO1L Upregulation in LTIH

Significant quantities of reactive oxygen species (ROS) can be produced within the endoplasmic reticulum (ER) during oxidative protein folding, and one of the sources of superoxide is ERO1L.<sup>33,34</sup> ERO1L transcription is upregulated by CHOP activation. To examine the ERO1L response to LTIH in motoneurons, we measured ERO1L mRNA in motor nuclei and immunodensity in motoneurons. Overall, there were significant genotype and LTIH effects,  $P = 0.005$ . In WT mice, there was a significant increase in ERO1L mRNA expression (normalized to  $10^6$  copies 18S mRNA) in the facial nucleus in LTIH-exposed mice ( $t = 3$ ,  $P < 0.05$ ), as summarized in Figure 6A. There was no effect of LTIH on ERO1L mRNA expression in CHOP-/- mice: CHOP-/- LTIH vs. CHOP-/- Sham mice,  $t = 1$ , N.S. We next evaluated the ERO1L protein expression in hypoglossal nucleus using the integrated density of immunofluorescence (Figure 6B and C). Most ERO1L labeling in the hypoglossal nucleus was in motoneurons, with very little in surrounding glia and dendrites (Figure 6C). ERO1L integrated immunodensity was significantly increased in WT LTIH mice ( $n = 5$ ) compared to Sham ( $n = 5$ ) ( $t = 8$ ,  $P < 0.001$ ). No significant difference in ERO1L protein expression was found between CHOP-/- LTIH and CHOP-/- Sham mice, as summarized in Figure 6B. As observed with mRNA, ERO1L protein was higher in WT LTIH than in CHOP-/- LTIH mice ( $t = 9$ ,  $P < 0.001$ ) (Figure 6B). Thus, in LTIH endogenous CHOP markedly upregulates ERO1L.

## Transgenic Absence of CHOP Prevents LTIH Induced Hypoglossal Motoneuron Apoptosis and Loss

Previously we showed that LTIH results in increased nuclear cleaved caspase-3 in hypoglossal motoneurons.<sup>21</sup> We first determined nuclear presence (% positive) of cleaved caspase-3 (CC-3) in WT and CHOP-/- mice exposed to Sham or LTIH for 12 wk ( $n = 5$ /group). Overall, there were significant LTIH and genotype effects ( $P = 0.0009$ ). An example is provided in Figure 7A. LTIH resulted in a large increase in nuclear CC-3 in WT mice ( $t = 5$ ,  $P < 0.001$ ); results are summarized in Figure 7B. In contrast, in CHOP-/- mice, CC-3 was not elevated by LTIH. CC-3 was greater in WT LTIH than in CHOP-/- LTIH ( $t = 3$ ,  $P < 0.05$ ). Because cleaved caspase-3 is also observed in neurites in response to neuronal signaling, we compared neuron counts in all groups to examine neuronal loss. Specifically, we counted nucleated ChAT-labeled and MAP-2 labeled large ( $> 20 \mu\text{m}$  diameter) neurons within the hypoglossal nucleus for each group. There were no differences in cell counts across WT mice and CHOP-/- mice exposed to Sham ( $t = 0.4$ , N.S.). LTIH resulted in a reduction of cells in the WT mice ( $t = 4$ ,  $P < 0.01$ ; Figure 7C), while there was no reduction in hypoglossal motoneurons on the CHOP-/- mice exposed to LTIH ( $t = 0.4$  N.S.). There were significant genotype effects of LTIH cell counts ( $t = 3$ ,  $P < 0.05$ ). Thus, transgenic absence of CHOP appears to prevent LTIH-induced apoptosis and neuronal loss in hypoglossal motoneurons.

## DISCUSSION

Obstructive sleep apnea is associated with injury to and dysfunction of peripheral nerves, including brainstem motoneurons.<sup>1</sup> Previously, we showed that LTIH, modeling OSA

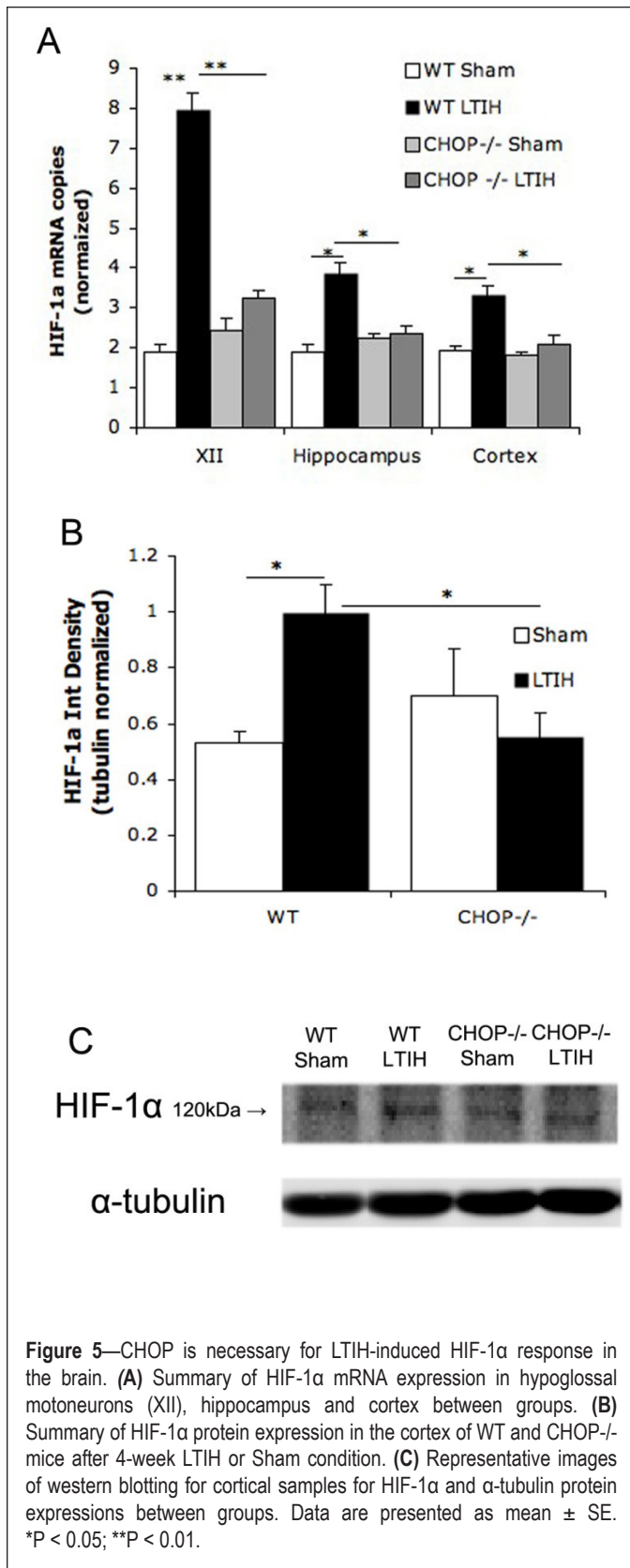


**Figure 5**—CHOP is necessary for LTIH-induced HIF-1α response in the brain. (A) Summary of HIF-1α mRNA expression in hypoglossal motoneurons (XII), hippocampus and cortex between groups. (B) Summary of HIF-1α protein expression in the cortex of WT and CHOP-/- mice after 4-week LTIH or Sham condition. (C) Representative images of western blotting for cortical samples for HIF-1α and α-tubulin protein expressions between groups. Data are presented as mean  $\pm$  SE. \* $P < 0.05$ ; \*\* $P < 0.01$ .

for HIF1α. As with mRNA, these were genotype and LTIH effects on HIF-1α protein (Figure 5B). Specifically, LTIH increased HIF-1α protein in the WT mice ( $t = 3$ ,  $P < 0.05$ ) but did not increase HIF-1α protein in the CHOP-/- mice (Figure 5B and C). This differential response resulted in increased HIF-1α in the WT mice relative to CHOP-/- mice ( $t = 3$ ,  $P < 0.05$ ).



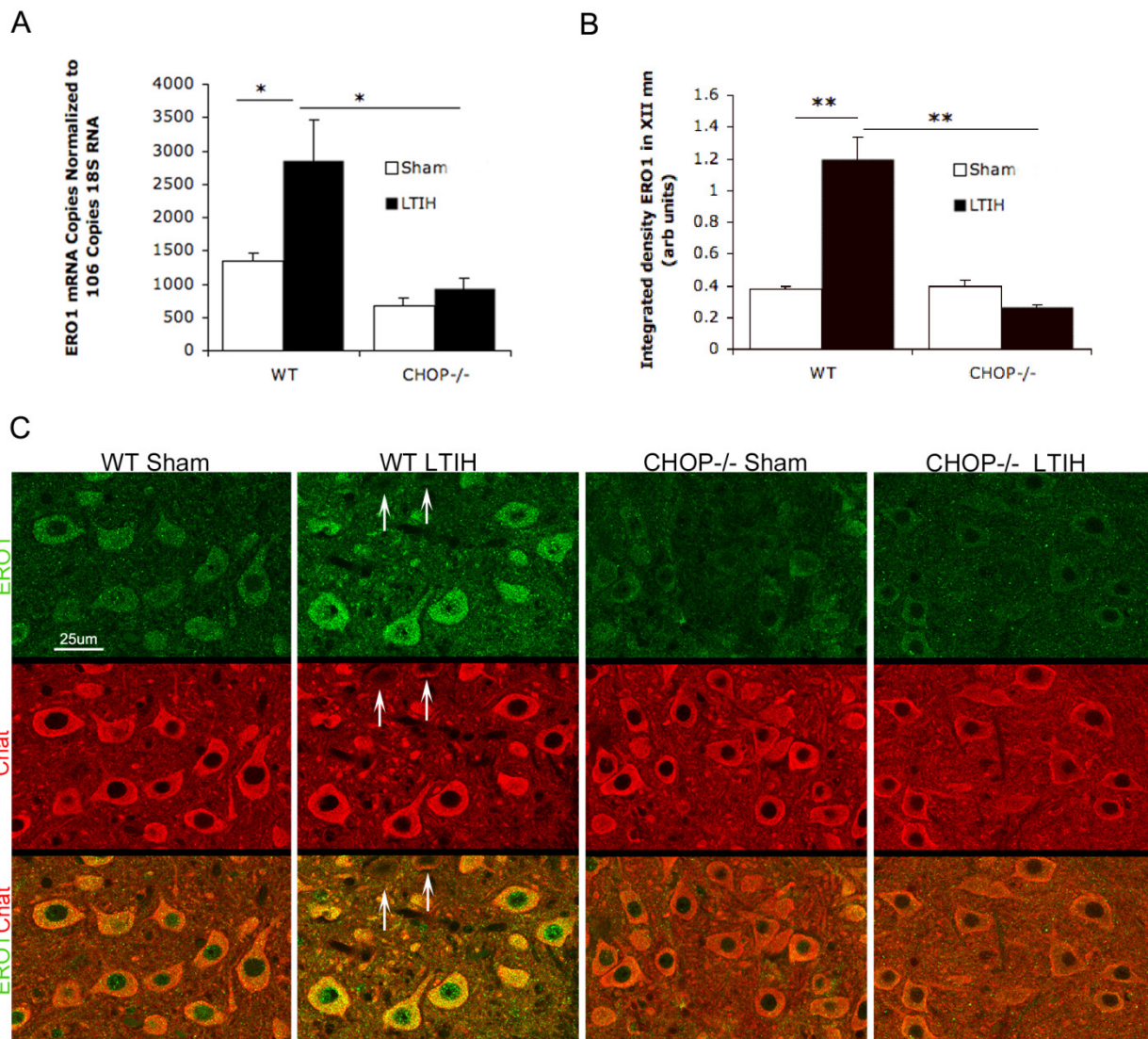


**Figure 6**—LTIH increases endoplasmic reticulum oxidoreductin 1 like protein (ERO1L), and is dependent upon the presence of CHOP. **(A)** Summary of ERO1L mRNA expression in facial neurons in WT and CHOP<sup>-/-</sup> mice with LTIH or sham LTIH. **(B)** Mean immunodensities for ERO1L expression in hypoglossal motoneurons between groups. **(C)** Sections of hypoglossal motoneurons with ERO1L (green color) and Chat (red color) labeling. Motoneurons weakly labeled with ChAT showed minimal ERO1L (arrows). Data are presented as mean ± SE. \*P < 0.05; \*\*P < 0.01. ChAT, choline acetyltransferase.

oxygenation patterns results in oxidative injury to and apoptosis in hypoglossal motoneurons and reduced excitation of the hypoglossal nerve.<sup>21,35</sup> Oxidative stress contributes to LTIH motoneuron injury. In support, administration of a superoxide dismutase mimetic across LTIH exposures reduces hypoglossal motoneuron injury and improves excitation of hypoglossal nerves.<sup>35</sup> LTIH, however, also results in significant ER stress with activation of CHOP and apoptosis pathways.<sup>21</sup> The purpose of the present work was to integrate the above oxidative and ER stress findings to determine whether ER stress influences oxidative stress in LTIH. Here we find that endogenous CHOP protein upregulates two major sources of reactive oxygen species in eukaryotic cells: NADPH oxidase and ERO1L. Moreover, endogenous CHOP contributes to LTIH superoxide production within brainstem motoneurons, as measured with dihydroethidium. Importantly, endogenous CHOP contributes

to both LTIH apoptosis and neuron loss, and CHOP plays similar roles in oxidative stress in other brain regions injured by LTIH, including the cortex and hippocampus. Collectively, the present data identify ER stress factor CHOP as a major contributor to LTIH oxidative neuronal injury and loss.

Nox2 is implicated in LTIH neural injuries, including cortical and hippocampal apoptosis. Nox2 upregulation in LTIH has also been shown to negatively influence spatial learning, memory, and wakefulness.<sup>15,30,32</sup> Moreover, Nox 2 is a major source of oxidative stress and neuroinflammation in response to intermittent hypoxia.<sup>15,18,19,30,36</sup> In this series of studies, we find that endogenous CHOP is responsible, at least in part, for Nox2 upregulation. In addition to CHOP upregulation of Nox2 mRNA and protein, we provide indirect evidence of CHOP effect on Nox2 activity in that CHOP<sup>-/-</sup> mice showed reduced LTIH superoxide production in neurons and carbonyl protein.

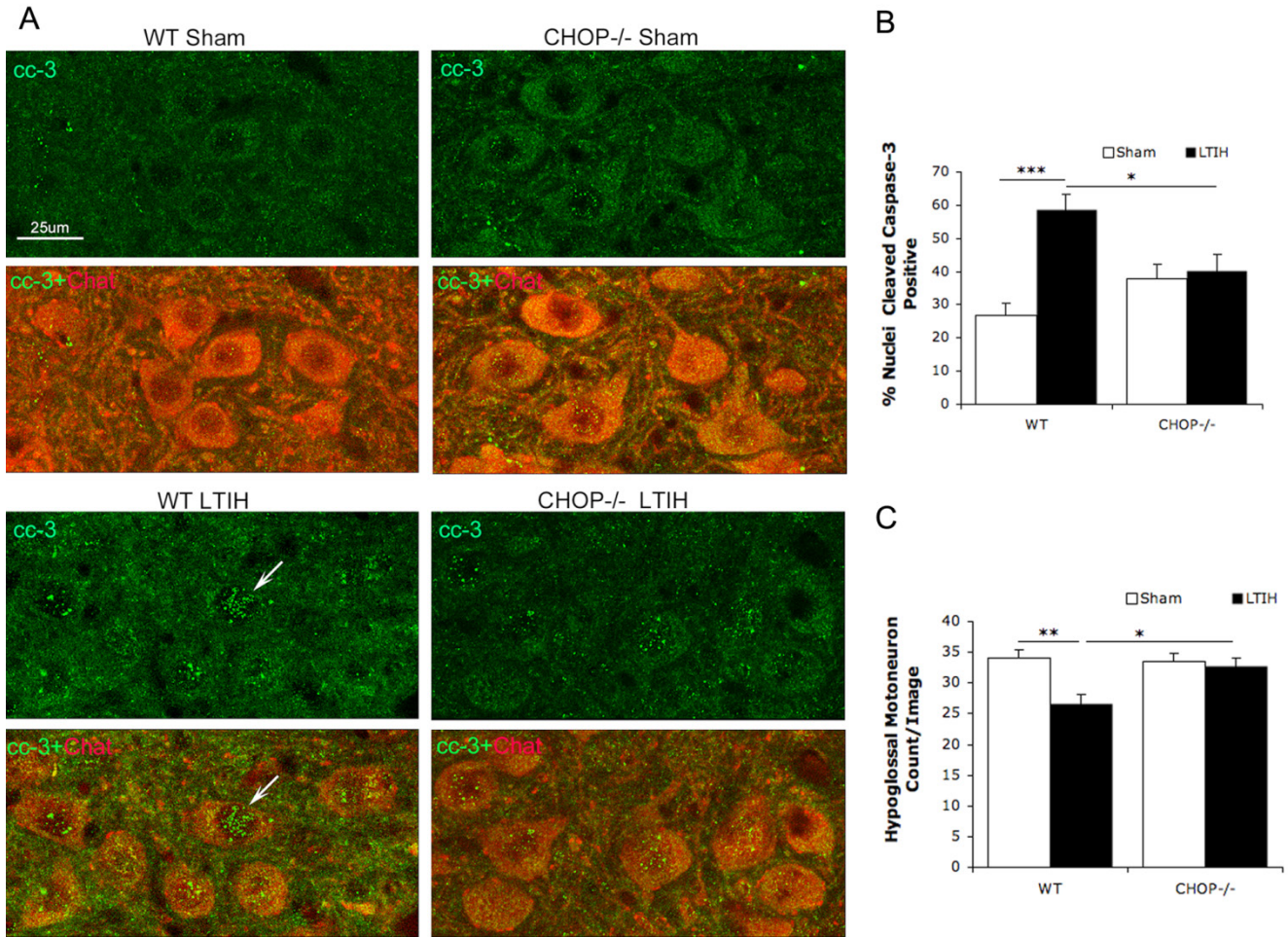


**Figure 7**—Effects of LTIH and CHOP on apoptosis in brainstem motoneurons. (A) Sections of hypoglossal motoneurons with CC-3 (green) and ChAT (red). There were more cells with CC-3 visible in motoneuron nuclei in WT LTIH mice than other groups, and some neurons with strong labeling (arrow). (B) Mean immunodensities for CC-3 expression in hypoglossal motoneuron nuclei between groups after 12-weeks exposure. (C) Summary of hypoglossal motoneuron counts between groups. Data presented as mean  $\pm$  SE. \* $P < 0.05$ ; \*\* $P < 0.01$ ; \*\*\* $P < 0.001$ . CC-3, cleaved caspase-3; Chat, choline acetyltransferase.

CHOP is activated by prolonged or severe ER stress, primarily through activation of the protein kinase R-like endoplasmic reticulum kinase (PERK) ER stress pathway.<sup>37</sup> Previously we identified activation of the PERK pathway in motoneurons in response to LTIH, where neurons with greater PERK activation under LTIH conditions expressed CHOP in response to LTIH.<sup>21</sup> Thus, Nox2 activation and upregulation in LTIH occur in part because of severe ER stress with CHOP activation.

Recent studies suggest that upregulation of HIF-1 $\alpha$  in intermittent hypoxia contributes to both oxidative stress and Nox2 upregulation and activation.<sup>17,38,39</sup> Intermittent hypoxia increases HIF-1 $\alpha$  mRNA and protein in response to oxidative stress.<sup>17,38</sup> Treatment with superoxide scavengers across exposure to intermittent hypoxia prevents HIF-1 $\alpha$  upregulation, while Nox2 inhibition or transgenic absence prevents HIF-1 $\alpha$  upregulation.<sup>17</sup> However, a more recent study has revealed a bi-directional relationship between HIF-1 $\alpha$  and Nox2 in that HIF-1 $\alpha$  is also necessary for the LTIH-induced Nox2 upregulation in both the forebrain (cortex) and brainstem.<sup>38</sup> The present studies identify CHOP as an upstream activator of the HIF-1 $\alpha$  transcriptional response to LTIH. Thus, activation of CHOP

triggers this feed-forward response between Nox2 and HIF-1 $\alpha$  increasing oxidative stress. Specifically, oxidative stress, in turn, promotes protein misfolding and further ER stress that, in turn, increases CHOP and oxidative stress.

Large neurons with extensive projections, including motoneurons and cortical and hippocampal pyramidal neurons, process immense amounts of membrane-bound and signaling proteins, that require folding in the ER. Folding of these proteins requires disulfide bond formation that can be an important source of oxidative stress.<sup>40</sup> ERO1 provides a disulfide relay to protein disulfide isomerase to introduce disulfide bonds into ER luminal proteins. ERO1L, a mammalian isoform, is a transcriptional target of HIF-1 $\alpha$ , and is upregulated in hypoxia presumably to prevent hypo-oxidation in the ER lumen. Under conditions of oxidative and/or ER stress, elevated levels of ERO1L activate the inositol 1,4,5-triphosphate (IP3) receptor (IP3R), increasing calcium release. ER-released cytosolic calcium activates Nox2 and several death effector pathways downstream of the calcium-activated Ca<sup>2+</sup>/calmodulin-dependent protein kinase II (CaMKII).<sup>41,42</sup> ER calcium release would also explain mitochondrial injury observed in LTIH.<sup>43</sup> Thus, ERO1L

introduces an additional Nox2 activation as illustrated in our proposed model in Figure 8. The precise steps (whether direct or indirect) whereby CHOP induces upregulation of Nox2, HIF-1 $\alpha$ , and ERO1L will require *in vitro* studies.

Although CHOP is frequently termed an apoptotic factor, the mechanisms by which CHOP contributes to apoptosis are incompletely understood. CHOP is increased under conditions of increased cellular stress and increased CHOP is evident during ER stress induced apoptosis.<sup>44</sup> Yet, overexpression of CHOP in otherwise healthy cells does not induce apoptosis or non-apoptotic cell death.<sup>45</sup> Consistent with our proposed model with CHOP positively influencing feed forward injuries, increased CHOP sensitizes eukaryotic cells to diverse physiological stressors.<sup>45</sup> Overexpression of CHOP dramatically suppresses BCL-2 transcription, and in doing so markedly reduces intracellular glutathione.<sup>45</sup> Reductions in glutathione would trigger increased oxidative stress responses to physiological perturbances. Here we find that transgenic ablation of CHOP improves neuronal outcomes, including survival, in LTIH.

While data for neural injury in sleep apnea are most compelling for peripheral nerve injury, there are many neurobehavioral impairments in sleep apnea that also improve with therapy, including deficits in short-term memory, fine motor control, mood, attention, and problem solving and sleepiness.<sup>1</sup> Whether mechanisms of injury in sleep apnea and in LTIH are similar or distinct across vulnerable brain regions has not been discerned. Inflammatory and oxidative stress responses have been seen in each region injured by LTIH, and Nox2 activation is central to oxidative and proinflammatory responses.<sup>15</sup> Here, we find that endogenous CHOP positively influences Nox2 and HIF-1 $\alpha$  upregulation in at least three major areas of injury, the brainstem motoneurons, cortex, and hippocampus, which might contribute to neurobehavioral impairments. This work supports the concept that CHOP would be an important pharmacological target to prevent sleep apnea neural injury in many brain regions and protect cognition.

The prevalence and severity of OSA rise with aging, obesity, and diabetes.<sup>46-48</sup> Yet we do not yet know whether any of these three conditions influences the neural outcomes for OSA beyond severity. All three conditions can increase ER stress and CHOP.<sup>49,50</sup> Thus, it is likely that there is additional neuronal injury in individuals with OSA and advanced aging, uncontrolled diabetes, and morbid obesity. Metformin, used to control glucose in type 2 diabetes, reduces ER stress and CHOP and has been shown to offer neuroprotection in some models of neuronal injury.<sup>51,52</sup> It will be of interest to determine whether metformin or GLP-1 agonists or any other drugs that reduce CHOP can protect against LTIH injury.

In conclusion, we show that endogenous CHOP influences oxidative stress, transcriptional regulation of HIF-1 $\alpha$ , Nox-2, and ERO1L apoptosis and neuronal loss in long-term intermittent hypoxia. The work provides an upstream target for preventing neuronal injury and neurobehavioral sequelae from intermittent hypoxia modeling sleep apnea.

#### ACKNOWLEDGMENTS

Work was performed at the University of Pennsylvania. The work was supported, in part, by NIH HLBI (HL079555, HL096037).

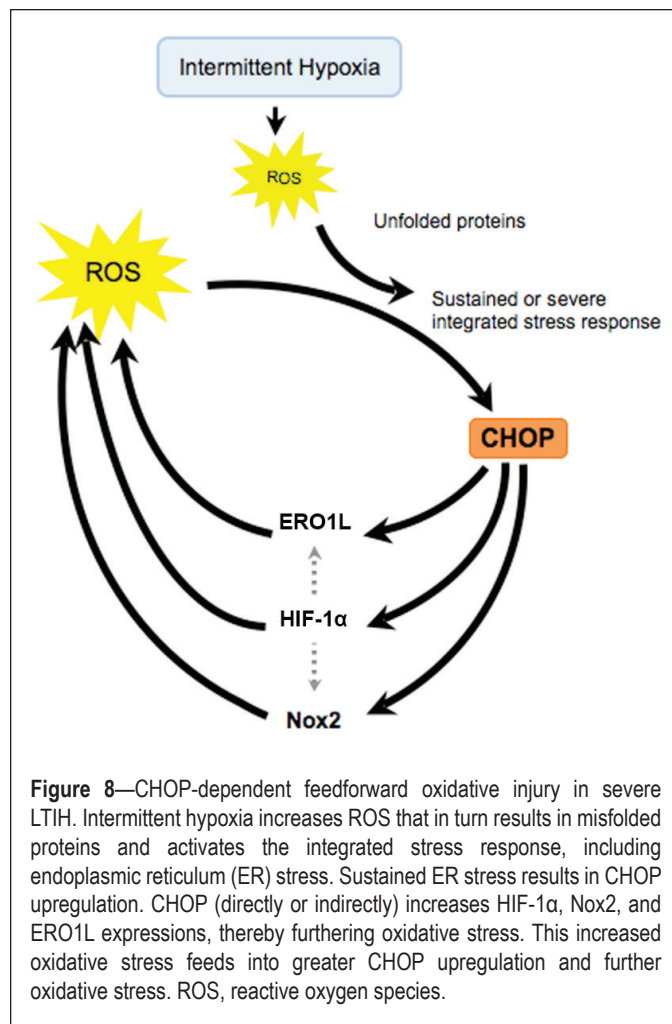


**Figure 8**—CHOP-dependent feedforward oxidative injury in severe LTIH. Intermittent hypoxia increases ROS that in turn results in misfolded proteins and activates the integrated stress response, including endoplasmic reticulum (ER) stress. Sustained ER stress results in CHOP upregulation. CHOP (directly or indirectly) increases HIF-1 $\alpha$ , Nox2, and ERO1L expressions, thereby furthering oxidative stress. This increased oxidative stress feeds into greater CHOP upregulation and further oxidative stress. ROS, reactive oxygen species.

Author's contributions: Dr. Chou: acquisition, analysis and interpretation of data for western blotting, quantitative real-time PCR and immunostaining studies, drafting the article; Dr. Zhan: design, acquisition and analysis of data for molecular studies; Dr. Zhu: acquisition and analysis of data for immunostaining studies; Polina Fenik: animal care, perfusion studies and tissue dissection; Dr. Panossian: acquisition and analysis of data for histologic studies; Dr. Li: acquisition and analysis of data for histologic studies; Dr. Zhang: animal care and acquisition data for molecular studies; Dr. Veasey: conception and design, analysis and interpretation of data, drafting and revising the article critically for important intellectual content

#### DISCLOSURE STATEMENT

This was not an industry supported study. The authors have indicated no financial conflicts of interest.

#### REFERENCES

1. Li Y, Veasey SC. Neurobiology and neuropathophysiology of obstructive sleep apnea. *Neuromolecular Med* 2012;14:168-79
2. Mayer P, Dematteis M, Pepin JL, et al. Peripheral neuropathy in sleep apnea. A tissue marker of the severity of nocturnal desaturation. *Am J Respir Crit Care Med* 1999;159:213-9.
3. Svanborg E. Upper airway nerve lesions in obstructive sleep apnea. *Am J Respir Crit Care Med* 2001;164:187-9.
4. Boyd JH, Petrof BJ, Hamid Q, Fraser R, Kimoff RJ. Upper airway muscle inflammation and denervation changes in obstructive sleep apnea. *Am J Respir Crit Care Med* 2004;170:541-6.

5. Friberg D, Ansved T, Borg K, Carlsson-Nordlander B, Larsson H, Svanborg E. Histological indications of a progressive snorers disease in an upper airway muscle. *Am J Respir Crit Care Med* 1998;157:586-93.
6. Remmers JE, deGroot WJ, Sauerland EK, Anch AM. Pathogenesis of upper airway occlusion during sleep. *J Appl Physiol* 1978;44:931-8.
7. Woodson BT, Garancis JC, Toohill RJ. Histopathologic changes in snoring and obstructive sleep apnea syndrome. *Laryngoscope* 1991;101:1318-22.
8. Friberg D, Gazelius B, Hokfelt T, Nordlander B. Abnormal afferent nerve endings in the soft palatal mucosa of sleep apnoics and habitual snorers. *Regul Pept* 1997;71:29-36.
9. Bassiouny A, Mashaly M, Nasr S, Atef A, Ayad E, Qotb M. Quantitative analysis of uvular muscles in cases of simple snoring and obstructive sleep apnea: an image analysis study. *Eur Arch Otorhinolaryngol* 2008;265:581-6.
10. Saboisky JP, Stashuk DW, Hamilton-Wright A, et al. Neurogenic changes in the upper airway of patients with obstructive sleep apnea. *Am J Respir Crit Care Med* 2012;185:322-9.
11. Ludemann P, Dziewas R, Soros P, Happe S, Frese A. Axonal polyneuropathy in obstructive sleep apnoea. *J Neurol Neurosurg Psychiatry* 2001;70:685-7.
12. Saboisky JP, Butler JE, McKenzie DK, et al. Neural drive to human genioglossus in obstructive sleep apnoea. *J Physiol* 2007;585:135-46.
13. Dziewas R, Schilling M, Engel P, et al. Treatment for obstructive sleep apnoea: effect on peripheral nerve function. *J Neurol Neurosurg Psychiatry* 2007;78:295-7.
14. Veasey SC, Davis CW, Fenik P, et al. Long-term intermittent hypoxia in mice: protracted hypersomnolence with oxidative injury to sleep-wake brain regions. *Sleep* 2004;27:194-201.
15. Zhan G, Serrano F, Fenik P, et al. NADPH oxidase mediates hypersomnolence and brain oxidative injury in a murine model of sleep apnea. *Am J Respir Crit Care Med* 2005;172:921-9.
16. Zhu Y, Fenik P, Zhan G, et al. Selective loss of catecholaminergic wake active neurons in a murine sleep apnea model. *J Neurosci* 2007;27:10060-71.
17. Yuan G, Nanduri J, Khan S, Semenza GL, Prabhakar NR. Induction of HIF-1 $\alpha$  expression by intermittent hypoxia: involvement of NADPH oxidase, Ca<sup>2+</sup> signaling, prolyl hydroxylases, and mTOR. *J Cell Physiol* 2008;217:674-85.
18. Nisbet RE, Graves AS, Kleinhenz DJ, et al. The role of NADPH oxidase in chronic intermittent hypoxia-induced pulmonary hypertension in mice. *Am J Respir Cell Mol Biol* 2009;40:601-9.
19. Khan SA, Nanduri J, Yuan G, et al. NADPH oxidase 2 mediates intermittent hypoxia-induced mitochondrial complex I inhibition: relevance to blood pressure changes in rats. *Antioxid Redox Signal* 2011;14:533-42.
20. Burckhardt IC, Gozal D, Dayyat E, et al. Green tea catechin polyphenols attenuate behavioral and oxidative responses to intermittent hypoxia. *Am J Respir Crit Care Med* 2008;177:1135-41.
21. Zhu Y, Fenik P, Zhan G, Sanfillipo-Cohn B, Naidoo N, Veasey SC. Eif-2 $\alpha$  protects brainstem motoneurons in a murine model of sleep apnea. *J Neurosci* 2008;28:2168-78.
22. Halterman MW, Gill M, DeJesus C, Ogihara M, Schor NF, Federoff HJ. The endoplasmic reticulum stress response factor CHOP-10 protects against hypoxia-induced neuronal death. *J Biol Chem* 2010;285:21329-40.
23. Ito Y, Yamada M, Tanaka H, et al. Involvement of CHOP, an ER-stress apoptotic mediator, in both human sporadic ALS and ALS model mice. *Neurobiol Dis* 2009;36:470-6.
24. Song B, Scheuner D, Ron D, Pennathur S, Kaufman RJ. Chop deletion reduces oxidative stress, improves beta cell function, and promotes cell survival in multiple mouse models of diabetes. *J Clin Invest* 2008;118:3378-89.
25. Prasanthi JR, Larson T, Schommer J, Ghribi O. Silencing GADD153/CHOP gene expression protects against Alzheimer's disease-like pathology induced by 27-hydroxycholesterol in rabbit hippocampus. *PLoS One* 2011;6:e26420.
26. Panossian L, Fenik P, Zhu Y, Zhan G, McBurney MW, Veasey S. SIRT1 Regulation of Wakefulness and Senescence-Like Phenotype in Wake Neurons. *J Neurosci* 2011;31:4025-36.
27. Zhao H, Joseph J, Fales HM, et al. Detection and characterization of the product of hydroethidine and intracellular superoxide by HPLC and limitations of fluorescence. *Proc Natl Acad Sci U S A* 2005;102:5727-32.
28. Barber RP, Phelps PE, Houser CR, Crawford GD, Salvaterra PM, Vaughn JE. The morphology and distribution of neurons containing choline acetyltransferase in the adult rat spinal cord: an immunocytochemical study. *J Comp Neurol* 1984;229:329-46.
29. Armstrong DM, Brady R, Hersh LB, Hayes RC, Wiley RG. Expression of choline acetyltransferase and nerve growth factor receptor within hypoglossal motoneurons following nerve injury. *J Comp Neurol* 1991;304:596-607.
30. Nair D, Dayyat EA, Zhang SX, Wang Y, Gozal D. Intermittent hypoxia-induced cognitive deficits are mediated by NADPH oxidase activity in a murine model of sleep apnea. *PLoS One* 2011;6:e19847.
31. Hui-guo L, Kui L, Yan-ning Z, Yong-jian X. Apocynin attenuate spatial learning deficits and oxidative responses to intermittent hypoxia. *Sleep Med* 2010;11:205-12.
32. Yuan G, Khan SA, Luo W, Nanduri J, Semenza GL, Prabhakar NR. Hypoxia-inducible factor 1 mediates increased expression of NADPH oxidase-2 in response to intermittent hypoxia. *J Cell Physiol* 2011;226:2925-33.
33. Harding HP, Zhang Y, Zeng H, et al. An integrated stress response regulates amino acid metabolism and resistance to oxidative stress. *Mol Cell* 2003;11:619-33.
34. Haynes CM, Titus EA, Cooper AA. Degradation of misfolded proteins prevents ER-derived oxidative stress and cell death. *Mol Cell* 2004;15:767-76.
35. Veasey SC, Zhan G, Fenik P, Pratico D. Long-term intermittent hypoxia: reduced excitatory hypoglossal nerve output. *Am J Respir Crit Care Med* 2004;170:665-72.
36. Hayashi T, Yamashita C, Matsumoto C, et al. Role of gp91phox-containing NADPH oxidase in left ventricular remodeling induced by intermittent hypoxic stress. *Am J Physiol Heart Circ Physiol* 2008;294:H2197-203.
37. Tabas I, Ron D. Integrating the mechanisms of apoptosis induced by endoplasmic reticulum stress. *Nat Cell Biol* 2011;13:184-90.
38. Yuan G, Khan SA, Luo W, Nanduri J, Semenza GL, Prabhakar NR. Hypoxia-inducible factor 1 mediates increased expression of NADPH oxidase-2 in response to intermittent hypoxia. *J Cell Physiol* 2011;226:2925-33.
39. Peng YJ, Yuan G, Ramakrishnan D, et al. Heterozygous HIF-1 $\alpha$  deficiency impairs carotid body-mediated systemic responses and reactive oxygen species generation in mice exposed to intermittent hypoxia. *J Physiol* 2006;577:705-16.
40. Shimizu Y, Hendershot LM. Oxidative folding: cellular strategies for dealing with the resultant equimolar production of reactive oxygen species. *Antioxid Redox Signal* 2009;11:2317-31.
41. Seimon TA, Obstfeld A, Moore KJ, Golenbock DT, Tabas I. Combinatorial pattern recognition receptor signaling alters the balance of life and death in macrophages. *Proc Natl Acad Sci U S A* 2006;103:19794-9.
42. Timmins JM, Ozcan L, Seimon TA, et al. Calcium/calmodulin-dependent protein kinase II links ER stress with Fas and mitochondrial apoptosis pathways. *J Clin Invest* 2009;119:2925-41.
43. Douglas RM, Ryu J, Kanaan A, et al. Neuronal death during combined intermittent hypoxia/hypercapnia is due to mitochondrial dysfunction. *Am J Physiol Cell Physiol* 2010;298:C1594-602.
44. Welihinda AA, Tirasophon W, Kaufman RJ. The cellular response to protein misfolding in the endoplasmic reticulum. *Gene Expr* 1999;7:293-300.
45. McCullough KD, Martindale JL, Klotz LO, Aw TY, Holbrook NJ. Gadd153 sensitizes cells to endoplasmic reticulum stress by down-regulating Bcl2 and perturbing the cellular redox state. *Mol Cell Biol* 2001;21:1249-59.
46. Ancoli-Israel S, Ayalon L. Diagnosis and treatment of sleep disorders in older adults. *Am J Geriatr Psychiatry* 2006;14:95-103.
47. Punjabi NM, Polotsky VY. Disorders of glucose metabolism in sleep apnea. *J Appl Physiol* 2005;99:1998-2007.
48. Akinnusi ME, Saliba R, Porhomayon J, El-Solh AA. Sleep disorders in morbid obesity. *Eur J Intern Med* 2012;23:219-26.
49. Cnop M, Fougelle F, Velloso LA. Endoplasmic reticulum stress, obesity and diabetes. *Trends Mol Med* 2012;18:59-68.
50. Naidoo N, Zhu J, Zhu Y, et al. Endoplasmic reticulum stress in wake-active neurons progresses with aging. *Aging Cell* 2011;10:640-9.
51. Jung TW, Lee MW, Lee YJ, Kim SM. Metformin prevents endoplasmic reticulum stress-induced apoptosis through AMPK-PI3K-c-Jun NH2 pathway. *Biochem Biophys Res Commun* 2012;417:147-52.
52. Pei L, Yang J, Du J, Liu H, Ao N, Zhang Y. Downregulation of chemerin and alleviation of endoplasmic reticulum stress by metformin in adipose tissue of rats. *Diabetes Res Clin Pract* 2012;97:267-75.